Scattering through fluids: speckle size measurement and Monte Carlo simulations close to and into the multiple scattering

Y. Piederrière, J. Cariou, Y. Guern, B. Le Jeune, G. Le Brun, J. Lotrian

Laboratoire de Spectrométrie et Optique Laser, U.F.R. Sciences
6, Avenue Le Gorgeu, BP 809, 29285 Brest Cedex,
Tel.: 33(0)2 98 01 66 30-Fax: 33(0)2 98 01 67 13
Yann.Piederriere@univ-brest.fr, Jack.Cariou@univ-brest.fr

Abstract: We report on measurements in transmission of the speckle produced by scattering liquid media: diluted milk and water solutions of polystyrene-microspheres of different diameters. The speckle size is affected not only by scattering parameters such as the optical thickness, but also by the dimensions of the scatters. From the speckle measurement, we propose a method to differentiate media. Moreover, a calculation of the transmitted light profile by Monte Carlo simulation allowed us to get a better insight on the speckle size evolution versus scattering.

OCIS codes: (030.6140) Speckle; (290.5850) Scattering, particle

References and links

1. J.W. Goodman, "Statistical Properties of Laser Speckle Patterns," in *Laser speckle and related phenomena*, Vol.9 in series Topics in Applied Physics, J.C. Dainty, Ed., (Springer-Verlag, Berlin, Heidelberg New York Tokyo, 1984).
2. J.H. Churnside and H.T. Yura, "Velocity measurement using laser speckle statistics," Appl. Opt. **20**, 3539-3541 (1981).
3. D.A. Boas and A. G. Yodh, "Spatially varying dynamical properties of turbid media probed with diffusing temporal light correlation," J. Opt. Soc. Am. A **14**, 192-215 (1997).
4. Y.Aizu, T.Asakura, "Bio-speckle phenomena and their application to the evaluation of blood flow," Opt. Las. Tech. **23**, 205-219 (1991).
5. I.V. Fedosov and V.V. Tuchin, "The use of dynamic speckle field space time correlation function estimates for the direction and velocity determination of blood flow," Proc. of SPIE **4434**, 192-196 (2001).
6. J.D. Briers, G. Richards and X.W. He, "Capillary blood flow monitoring using laser speckle contrast analysis (LASCA)," J. Biomed. Opt. **4**, 164-175 (1999).
7. D.A. Zimnyakov, J.D. Briers, V.V. Tuchin, "Speckle technologies for monitoring and imaging of tissues and tissuelike phantoms," Chap.18 in *Handbook of biomedical diagnostics*, Valery V. Tuchin, Ed. (SPIE press, Bellingham 2002).
8. P. Lehmann, "Surface-roughness measurement based on the intensity correlation function of scattered light under speckle-pattern illumination," Appl. Opt. **38**, 1144-1152 (1999).
9. G. Da Costa and J. Ferrari, "Anisotropic speckle patterns in the light scattered by rough cylindrical surfaces," Appl. Opt. **36**, 5231-5237 (1997).
10. R. Berlasso, F. Perez Quintian, M.A. Rebollo, C.A. Raffo and N.G. Gaggioli, "Study of speckle size of light scattered from cylindrical rough surfaces," Appl. Opt. **39**, 5811-5819 (2000).
11. A. Sadhwani, K.T. Schomaker, G.J. Tearney and N.S. Nishioka, "Determination of Teflon thickness with laser speckle. I. Potential for burn depth diagnosis," Appl. Opt. **35**, 5727-5735 (1996).
12. M. Giglio, M. Carpineti, A. Vailati and D. Brogioli, "Near-field intensity correlation of scattered light," Appl. Opt. **40**, 4036-4040 (2001).
13. N.L. Swanson, B.D. Billard, and T.L. Gennaro, "Limits of optical transmission measurements with application to particle sizing techniques," Appl. Opt. **38**, 5887-5893 (1999).
14. H.C. Van de Hulst, *Light scattering by small particles* (New York, Dover, 1981).
15. G. Yoon, S.A. Prahl and A.J. Welch, "Accuracies of the diffusion approximation and its similarity relations for laser irradiated biological media," Appl. Opt. **28**, 2250-2255 (1989).

#3393 - $15.00 US Received 20 November 2003; revised 19 December 2003; accepted 27 December 2003

16. Terri L. Alexander, James E. Harvey, and Arthur R. Weeks, "Average speckle size as a function of intensity threshold level: comparison of experimental measurements with theory," Appl. Opt. **33**, 8240-8250 (1994).
17. C.A. Thompson, K.J. Webb, and A.M. Weiner, "Imaging in scattering media by use of laser speckle," J. Opt. Soc. Am. A **14**, 2269-2277 (1997).

1. Introduction

Laser light-induced granularity can be observed either in free space (objective speckle) or on the image plane of a diffuse object illuminated by a coherent source (subjective speckle) [1]. The speckle effect through a coherent light source-illuminated medium results from random fluctuations of refractive index (Fig. 1). Photons travel along random optical paths; the random dephasing of associated wavelets produce random interferences that induce a statistical distribution of light intensity.

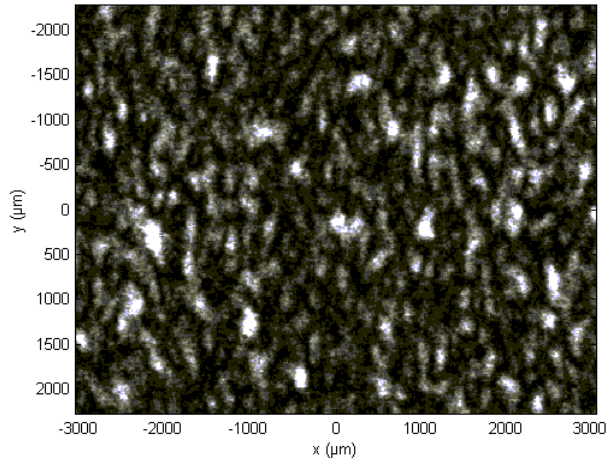

Fig. 1. Speckle produced by a weak diffusing medium.

Speckle parameters (size, contrast, intensity, polarization,…) can bring information on scattering media. Dynamical speckle analysis has become a current method to characterize the dynamic behavior of scattering medium such as flow or Brownian movement. The motion of the speckle field is analyzed by correlometric methods [2,3,4,5] or laser speckle contrast measurement [6,7]. Spatial characteristics such as the speckle size can be used to measure the roughness of surfaces [8,9,10] or to determinate the thickness of Teflon plate for example [11]. These experiments generally use the backscattered speckle configuration. In transmission, Marzio Giglio *et al.* [12] proposed an optical set-up to measure the correlation function in the near field, and show the near-field speckle dependence on the particles size.

So, under some conditions, the speckle size depends on different optical parameters of the media of concern. The determination of these parameters can be necessary for optical application in medical diagnosis, for example. Here, we measured the evolution of speckle size versus the scattering effects, in transmission, induced by the optical thickness and particles size of the media. We calculated the spatial intensity profile of a scattered beam at the output surface of a scattering sample thanks to Monte Carlo simulation and deduced the evolution of the speckle size from its power spectral density.

#3393 - $15.00 US Received 20 November 2003; revised 19 December 2003; accepted 27 December 2003

2. The radiative transport equation

Random media can be characterized by their scattering and absorption coefficients usually denoted μ_s and μ_a, respectively. If absorption is very weak compared to scattering and that the light crosses a slab of thickness *L*, the optical thickness $ls = L\mu_s$ is used to define the scattering regime [13].

The choice of an appropriate theory to describe light transmission through an attenuating medium depends on the concentration of attenuating particles. When this concentration is low (single scattering, $ls < 1$), the Mie theory explains light propagation [14].
The light propagation is governed by the Radiative Transfert Equation (RTE) when the concentration of particle is increased (multiple scattering, $1 < ls < 10$).
When the concentration is very high ($ls > 10$), photons undergo a random walk in the medium, and the light propagation is specified by the diffusion approximation to the RTE [15].

In our case-study, the light was affected by multiple and single scattering; a solution to the RTE was, therefore, needed to describe the transport of photons in the medium. In the absence of source terms, the RTE is written as [13]:

$$\frac{\partial P(r,q)}{\partial s} = -\mu_t P(r,q) + \frac{\mu_s}{4\pi}\int_{4\pi} P(r,q')\beta(q,q')d\Omega' \qquad (1)$$

where $P(r,q)$ is the monochromatic radiance at a point *r* in the direction *q*, $d\Omega'$ is the unit solid angle around the direction q', $\beta(q,q')$ is the normalized scattering phase function, which describes the scattering properties of medium and represents the probability density function of photon scattering from the direction q to direction q', $\mu_t = \mu_a + \mu_s$ (in m^{-1}) is the total attenuation coefficient produced by absorption and scattering. The left side of Eq.(1) is the change in intensity as the light traverses the medium. The first term, $-\mu_t P(r,q)$, represents absorption and scattering losses, whereas the second term expresses the fraction of the total scattered light collected within the solid angle of the detector.

A solution of the RTE was calculated by Monte Carlo simulation where the scattering phase functions were determined from the Mie Theory by using the refractive index and the particles size-distribution. We, thus, obtained the light distribution after the diffusing medium versus the refractive indices of the particles and medium, the wavelength, the medium thickness, the laser beam width and the particle size-distribution.

3. Speckle size

To estimate the speckle size, we calculated the normalized autocovariance function of the intensity speckle pattern obtained in the observation plane (x, y). This function corresponds to the normalized autocorrelation function of the intensity; it has a zero base and its width provides a reasonable measurement of the "average width" of a speckle [1]. If $I(x_1, y_1)$ and $I(x_2, y_2)$ are the intensities of two points in the observation plane (x, y), the intensity autocorrelation function is defined by Eq. (2) [1]:

$$R_I(\Delta x, \Delta y) = \langle I(x_1, y_1) I(x_2, y_2) \rangle \qquad (2)$$

where $\Delta x = x_1 - x_2$ and $\Delta y = y_1 - y_2$. $\langle\ \rangle$ corresponds to a spatial average. If $x_2 = 0$, $y_2 = 0$, $x_1 = x$ and $y_1 = y$, we can write:

#3393 - $15.00 US Received 20 November 2003; revised 19 December 2003; accepted 27 December 2003

$$R_I(\Delta x, \Delta y) = R_I(x, y) \tag{3}$$

The normalized autocovariance function of the intensity, $c_I(x, y)$, is given by Eq. (4):

$$c_I(x, y) = \frac{R_I(x, y) - \langle I(x, y) \rangle^2}{\langle I(x, y)^2 \rangle - \langle I(x, y) \rangle^2} \tag{4}$$

In this study we calculated $c_I(x, y)$ by two methods. The first one allows the calculation of the normalized autocovariance function from the measured intensity distribution of the speckle. Let us call c_I^m the normalized autocovariance function given by this method, *m* suffix corresponds to "measured". The second method determines also the normalized autocovariance function, but from the calculation of the spatial intensity profile of the scattered beam at the output surface of the scattering medium. Its result is denoted c_I^c where *c* suffix corresponds to "calculated". The spatial intensity profile was deduced from Monte Carlo simulation, and thus c_I^c corresponds to the theoretical prediction of c_I^m.

3.1 c_I^m calculation

As implied by the Wiener-Khintchine theorem, the autocorrelation function of the intensity is given by the Inverse Fourier Transform (FT^{-1}) of the Power Spectral Density (*PSD*) of the intensity:

$$R_I(x, y) = FT^{-1}\left[PSD_I(\upsilon_x, \upsilon_y) \right] \tag{5}$$

with:

$$PSD_I(\upsilon_x, \upsilon_y) = \left| FT\left[I(x, y) \right] \right|^2 \tag{6}$$

FT is the Fourier Transform.

$c_I^m(x, y)$ calculated from the intensity distribution measured of the speckle is:

$$c_I^m(x, y) = \frac{FT^{-1}\left[\left| FT\left[I(x, y) \right] \right|^2 \right] - \langle I(x, y) \rangle^2}{\langle I(x, y)^2 \rangle - \langle I(x, y) \rangle^2} \tag{7}$$

$c_I^m(x, 0)$ and $c_I^m(0, y)$ are the horizontal and the vertical profile of $c_I^m(x, y)$, respectively. Let us term dx^m the width of $c_I^m(x, 0)$ so that $c_I^m(dx^m / 2, 0) = 0.5$ (see figure 2) and dy^m the width of $c_I^m(0, y)$ such as $c_I^m(0, dy^m / 2) = 0.5$. Both parameters, dx^m and dy^m, allowed us to measure the horizontal and vertical speckle size.

#3393 - $15.00 US Received 20 November 2003; revised 19 December 2003; accepted 27 December 2003

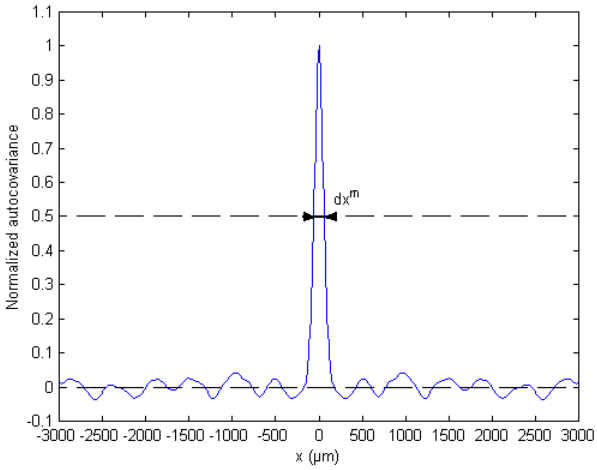

Fig. 2. $c_I^m(x,0)$ calculated from speckle of fig. 1.

3.2 c_I^c calculation

In the case of a diffusing surface we have [1]:

$$R_I(x,y) = \langle I \rangle^2 \left[1 + \left| \mu_A(x,y) \right|^2 \right] \tag{8}$$

where $\left| \mu_A(x,y) \right|^2$ is the squared complex coherence factor and corresponds to $c_I(x,y)$. $\left| \mu_A(x,y) \right|^2$ is given by the Power Spectral Density of the illuminated area; this result ensues from the Van Cittert-Zernike (VCZ) theorem [12]:

$$\left| \mu_A(x,y) \right|^2 = \left| \frac{\int_{-\infty}^{\infty}\int_{-\infty}^{\infty} P(u,v) \exp\left[i \frac{2\pi}{\lambda z}(ux+vy) \right] dudv}{\int_{-\infty}^{\infty}\int_{-\infty}^{\infty} P(u,v) dudv} \right|^2 = c_I(x,y) \tag{9}$$

where (u,v) is the plane of the output surface of the scattering sample, λ is the wavelength, $z = D$ is the distance between the output surface of the scattering sample and the observation plane on the detector and $P(u,v)$ is the beam intensity distribution.
With the spatial frequencies, X and Y:

$$\begin{cases} X = \dfrac{x}{\lambda z} \\ Y = \dfrac{y}{\lambda z} \end{cases} \tag{10}$$

we have:

#3393 - $15.00 US Received 20 November 2003; revised 19 December 2003; accepted 27 December 2003

$$c_I(x,y) = \frac{\left|Fp(X,Y)\right|^2}{\left|\int_{-\infty}^{\infty}\int_{-\infty}^{\infty} P(u,v)dudv\right|^2} \tag{11}$$

where $Fp(X,Y)$ is the Fourier Transform of the light spatial intensity profile:

$$Fp(X,Y) = \int_{-\infty}^{\infty}\int_{-\infty}^{\infty} P(u,v)\exp\left[i2\pi\left(uX+vY\right)\right]dudv \tag{12}$$

By analogy, we calculated the light spatial intensity profile, $P(u,v)$, at the output surface of the scattering sample by the Monte-Carlo method. Since the optical axis is the laser beam direction, $P(u,v)$ is symmetric by revolution around this axis, and thus we get $c_I^c(x)$ as follows:

$$c_I^c(x) = \frac{\left|Fp(X)\right|^2}{\left|\int_{-\infty}^{\infty} P(u)du\right|^2} \tag{13}$$

Let us denote d^c the width of $c_I^c(x)$ so that $c_I^c(d^c/2) = 0.5$ and in order to compare it with dy^m. The following sections will, thus, deal with the measurement, calculation and evolution of the speckle size versus the optical thickness for different sizes of particles contained in the media.

4. Material and method

Figure 3 illustrates the experimental set up. The 7- mW HeNe laser used emits a 1.12 mm-wide polarized (linear) beam at I_0/e^2 with I_0 being the maximum laser intensity, at the 632.8 nm wavelength with a coherence length of about 20 cm. The light intensity is monitored by a half wave plate L associated to a polarizer P1. The length L of the fluid sample is 2 cm.

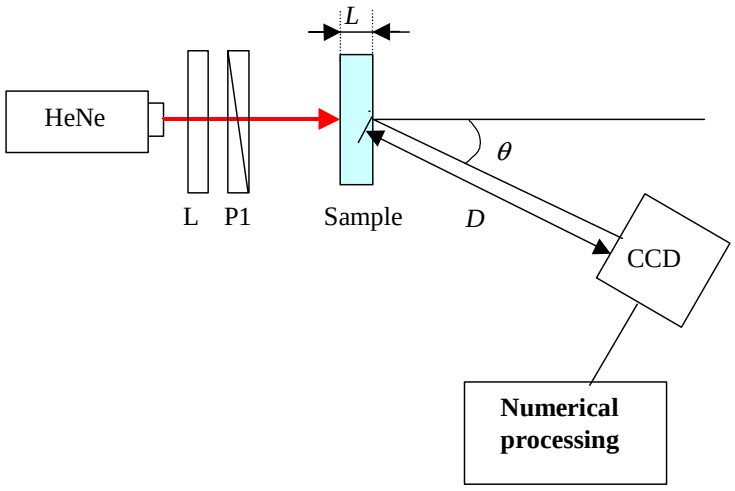

Fig. 3. Experimental set-up (top view).

#3393 - $15.00 US Received 20 November 2003; revised 19 December 2003; accepted 27 December 2003

To carry out our experiments the scattering media were prepared with deionized water mixed with either semi-skimmed milk, or skimmed milk, or polystyrene-microspheres of different diameters from Polyscience Inc.; these microspheres are provided in deionized water solutions and their number per cubed meter, *N*, is known. Furthermore, we used deionized water to avoid the possible effect of electrostatic interaction-caused particle aggregation. A CCD camera records the medium-produced speckle field. The CCD imager contains 788×268 pixels that are 8 µm×8 µm in size. When a newly acquired image is digitized, the analog-to-digital converter assigns an intensity value (gray level) in the range of 1 to 1024 (10-bit precision).

To record the speckle, one should be aware of the Brownian motion of particles in the medium. These movement induce a random agitation of the speckle ("boiling speckle"). Consequently, the image acquisition time must be very short. So, the time exposure of our CCD camera could vary from 60.10^{-3} to 10^{-4} s. However, in order to keep a correct signal-to-noise ratio, in our experiments image acquisition took 0.001 s.

Another consideration of importance in recording the speckle data is the speckle size on the CCD array: the speckles must be large as compared to the pixel size so as to resolve variations in speckle intensity [16]. Moreover, each image needs to contain many speckles for meaningful statistical evaluation. These conditions were met by choosing the distance *D* (*D* = 36 cm) between the sample and the CCD camera.

In order not to record the directly transmitted laser beam the CCD camera is positioned at an angle θ with the optical axis (Fig. 3). Figures 4 and 5 respectively depict the variations of the speckle size, i.e. dx^m and dy^m versus θ. Contrarily to dx^m, when $\theta < 10°$ dy^m variation versus θ is small. In our experiments $\theta = 5°$, so we made the following approximation:

$$dy^m(\theta = 5°) \sim dy^m(\theta = 0°)$$

But, as the angle of observation is not taken into account in d^c calculation, we considered that $\theta = 0°$, and consequently compared dy^m with d^c.

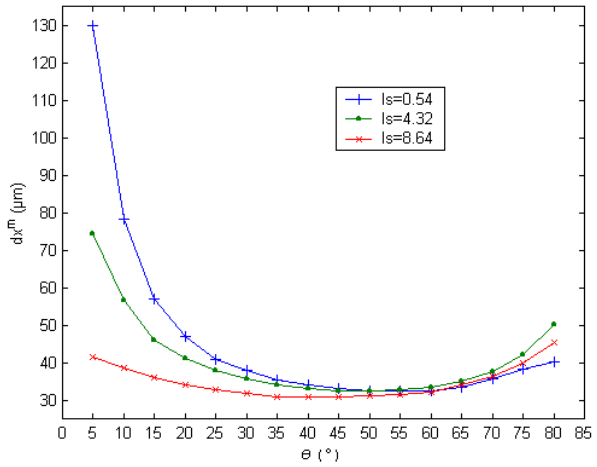

Fig. 4. dx^m versus θ.

#3393 - $15.00 US Received 20 November 2003; revised 19 December 2003; accepted 27 December 2003

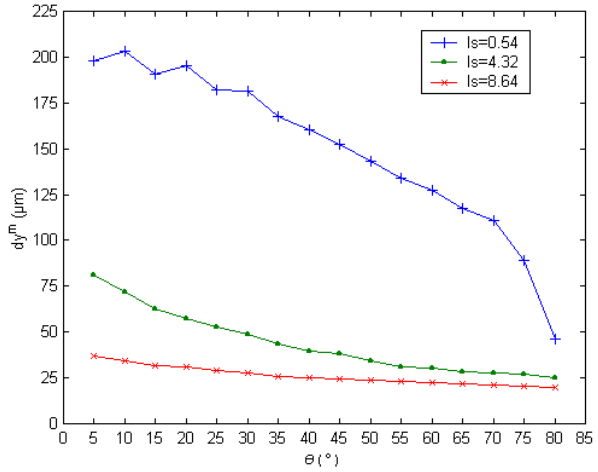

Fig. 5. dy^m versus θ.

Furthermore, since any change in milk concentration affects its scattering coefficient μ_s, we measured μ_s with respect to the milk concentration c in percent. It was found to be $2.16\,c$ and $0.39\,c.\text{cm}^{-1}$ for semi-skimmed and skimmed milks, respectively. For polystyrene microspheres and at the wavelength used, the absorption coefficient is insignificant as compared to the scattering one, which allows the measurement of scattering coefficient from the Beer Lambert law [13]. Table 1 gives the scattering coefficients we measured with respect to c with a ±5% precision as well as the particle diameters ∅ and the number of particles per cubed meter, N. The anisotropy factor g issued from the Monte Carlo simulation is shown in Table 2. The refractive indices used were 1.59 and 1.33 for the for the spheres and medium, respectively.

Table1. Scattering coefficients of polystyrene microspheres measured.

∅ (µm)	N (m^{-3}) (c=100%)	μ_s (cm^{-1})
0.20	$5.759*10^{16}$	$1.8c$
0.53	$3.147*10^{15}$	$6.23c$
1.44	$1.705*10^{14}$	$9.3c$
3.17	$1.484*10^{13}$	$2.15c$
6.36	$1.873*10^{12}$	$1.43c$

Table 2. Anisotropy factor of polystyrene microspheres calculated.

∅ (µm)	g
0.20	0.323
0.53	0.838
1.44	0.928
3.17	0.826
6.36	0.823

#3393 - $15.00 US Received 20 November 2003; revised 19 December 2003; accepted 27 December 2003

5. Results and discussions

Figure 6 depicts dy^m evolution versus *ls*, the optical thickness, for semi-skimmed milk. It clearly shows a linear section at low scattering, *ls* < 4.9. The fit of this part gives:

$$dy^m = -30ls + 219$$

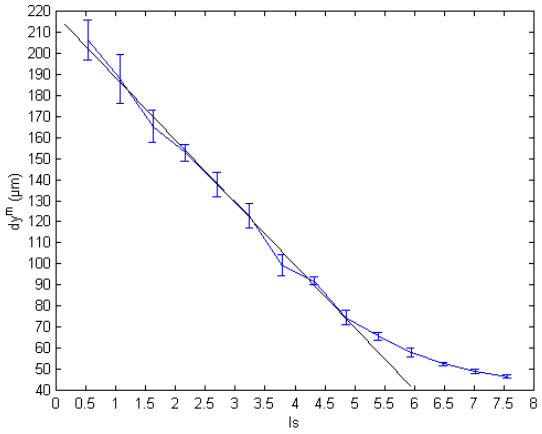

Fig. 6. dy^m versus *ls*, the opticalthickness for semi-skimmed milk.

A similar evolution is evidenced for skimmed milk in Fig. 7. The fit of the linear part gives:

$$dy^m = -48ls + 228$$

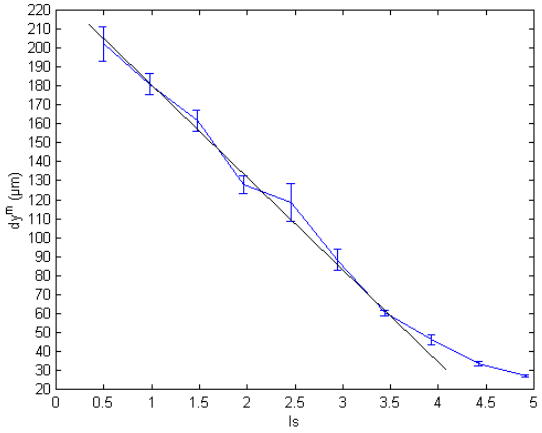

Fig. 7. dy^m versus *ls*, the optical thickness for skimmed milk.

We also calculated d^c for a typical size distribution of skimmed-milk particles and plotted it versus *ls* (Fig.8). Once again the plot highlights a linear section where:

$$d^c = -66ls + 216$$

#3393 - $15.00 US Received 20 November 2003; revised 19 December 2003; accepted 27 December 2003

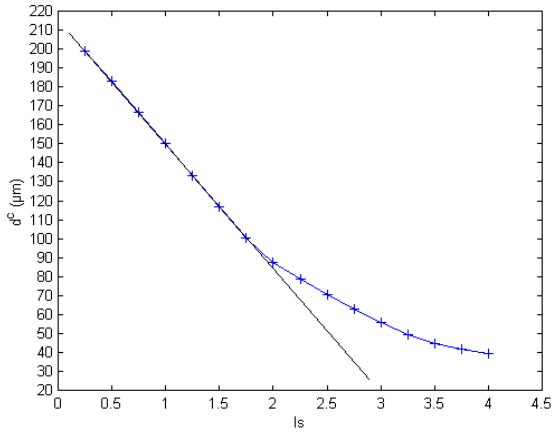

Fig. 8. d^c versus ls for skimmed milk.

This result evidences some linearity in the speckle size evolution at low scattering. Moreover, it is worth noting that the changes in speckle size are limited when $ls > 4$ for the skimmed milk and when $ls > 2$ for the d^c calculation.

If we call a^m the absolute value of the angular coefficient of the linear fit of dy^m, it is worth noting that it is smaller for the semi-skimmed milk than for the skimmed one ($a^m = 30$ and $a^m = 48$ respectively). This difference may result from disparity in the size distribution function of the milk particles.

To get a better insight on this issue, we conducted similar experiments on polystyrene-microspheres of different diameters in water solution. Figure 9 illustrates dy^m evolution versus ls and the linear fits for these polystyrene-microsphere media.

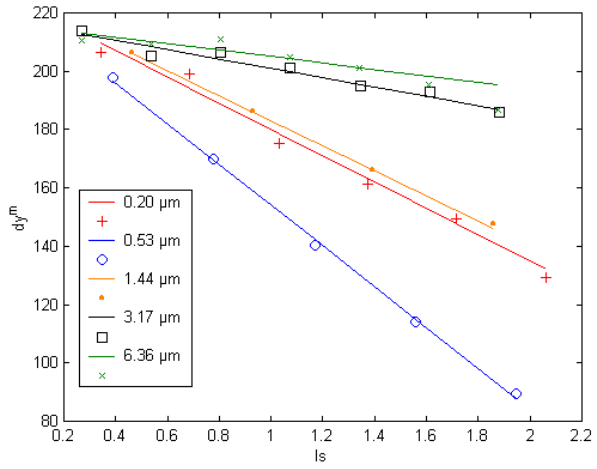

Fig.9. dy^m versus ls and linear fit for different polystyrene-microspheres.

For $ls < 2$, Table 3 lists the linear fit, dy^m issued from Fig.9.

#3393 - $15.00 US Received 20 November 2003; revised 19 December 2003; accepted 27 December 2003

Table 3. Parameters obtained with the proposed method for polystyrene microspheres.

	Measured	Calculated	
	Fig.9	Fig.11	
∅ (µm)	dy^m (µm)	d^c (µm)	d^{c2} (µm)
0.20	-45*ls* + 225	×	-15*ls* + 210
0.53	-70*ls* + 224	×	-41*ls* + 214
1.44	-43*ls* + 226	-71*ls* + 218	-55*ls* + 207
3.17	-16*ls* + 217	-49*ls* + 216	-43*ls* + 208
6.36	-11*ls* + 216	-41*ls* + 214	-32*ls* + 205

For particle diameters within 0.53 and 6.36 µm, a^m decreases with increasing diameter; this effect is more noticeable within 0.53 and 3.17 µm. Thus, at a given optical thickness, the speckle size is increasing concomitantly with the scatters size.

One should note in Table 3 that the 0.20-µm microspheres and the 1.44-µm ones produced alike results; this means that both sizes of particles produce the same speckle size for the same optical thickness. However, Fig. 10 highlights that the use of Eq (14) allows one to differentiate these media through contrast speckle measurement.

$$C = \frac{\sqrt{\left\langle I^2(x,y)\right\rangle - \left\langle I(x,y)\right\rangle^2}}{\left\langle I(x,y)\right\rangle} \tag{14}$$

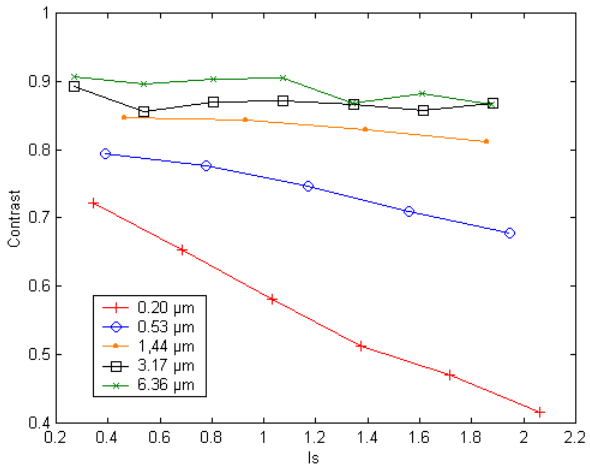

Fig. 10. Contrast evolution versus *ls* for different polystyrene-microspheres.

The calculated contrast, *C*, for the small spheres is far much lower than those of the other spheres. It ensues that the stray light, which is not implicated in the speckle formation, should be more important when the spheres are small. A large CCD acquisition time can affect the measured contrast since the speckle can move during the time needed for image acquisition. In our study, we verified that the acquisition time of 0.001 s is short enough to ignore the effects of speckle dynamics even for the 0.20 µm microspheres. So, any damage in contrast may be caused by the depolarization effect, by decoherence effect…

Figure 11 gives the calculated d^c for all the microspheres.

#3393 - $15.00 US Received 20 November 2003; revised 19 December 2003; accepted 27 December 2003

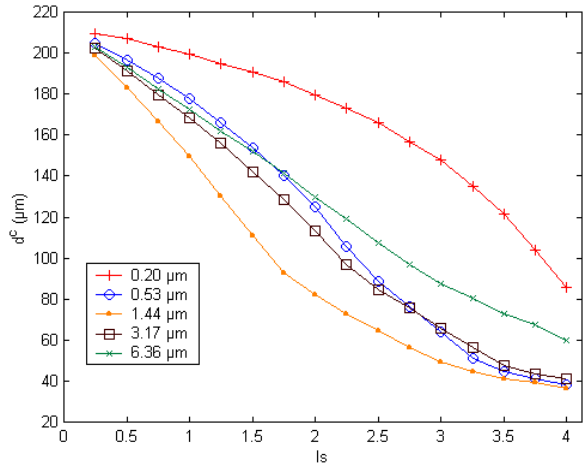

Fig. 11. d^c versus ls for the polystyrene-microspheres.

Table 3 gives the linear fits for the 1.44-, 3.17-, and 6.36-µm-diameter microspheres when $ls < 2$; the absolute value of the angular coefficient is denoted a^c. The results for the 0.20-, and 0.53-µm-diameter microspheres are missing of the Table 1, because the linear fits of d^c is impossible for these diameters when $0 < ls < 2$.

Table 3 evidences that, in the range 1.44 - 6.36 µm, a^c is decreasing when the diameter is increasing. However, the 0.53-µm diameter disagrees with this evolution; for $ls < 1.6$, $d^c(\varnothing = 0.53) > d^c(\varnothing = 6.36)$ (see Fig. 11).

Thus, within 6.36 - 1.44 µm, the theoretical approach permitted us to predict an a^m increase concomitant with a diameter reduction in agreement with measurements. Moreover, for small microspheres, the measured data and those issued from calculation both evidenced disagreement with this evolution. The differences observed between a^m and a^c values led us to wonder which photons of the profile are at the origin of the speckle. Indeed, no speckle was measured when the polarizer crossed the linear polarization of the laser beam, and therefore, the observed speckle was polarized. The intensity of any polarized profile can be calculated provided that the multiple scattering-depolarized photons are removed. This consideration led us to approximate that all the photons scattered more than two times were out of the simulated profile *P*. We thus denoted *P'* the new simulated profile, and calculated the new values of d^c denoted d^{c2}. Table 3 gives the linear fits obtained under this condition and shows that for the 1.44-, 3.17-, and 6.36-µm-diameter microspheres, the calculated a^{c2} are closer to the coefficients a^m issued from dy^m calculation. The agreement between calculation and measurement is better than above.

Moreover, in Table 3 for $ls \longrightarrow 0$ we observe that dy^m and d^c results are similar and are not depend on the microsphere size. In this case, the VCZ theorem can be strictly applied with the intensity distribution of the laser beam at the exit of the medium but the discrepancy increases concomitantly with *ls*.

#3393 - $15.00 US Received 20 November 2003; revised 19 December 2003; accepted 27 December 2003

6. Conclusion

In this study about the speckle produced in transmission by scattering fluid media, we measured the evolution of its size versus the optical thickness and the particle size in the media. At weak scattering the speckle size decreases linearly with the scattering. Moreover, for the biggest particles and a fixed optical thickness, the speckle size increases concomitantly with the particle diameter. This variation was measured for diameters within 0.53 and 6.36 µm. But, we noticed that media composed of either small particles or large ones can produce the same size of speckle. Consequently, another parameter is necessary to distinguish among them. We show that it may be the speckle contrast, which is weaker for small particles than for big ones. Furthermore, in the case of a large optical path length as compared to the laser coherence length, the speckle contrast is known to decrease [17]. Ongoing simulations within our laboratory focus on the calculation of this optical path length to explain the contrast difference displayed by small particles.

Our theoretical approach considered a scattering-induced widening of the transmitted laser beam. We, therefore, calculated the intensity of the transmitted light by Monte Carlo method. The speckle size was determined from this intensity profile. Its linear evolution, before a "saturation" of the speckle size versus scattering, was also evidenced from calculation under weak scattering condition. The effect of the particle size was calculated too: for diameter in the range 1.44 - 6.36 µm, the speckle size increased concomitantly with the particle dimension. On the other hand for small particles, calculation showed a different evolution: the speckle size increased with decreasing diameter. Calculation is, therefore, insufficient for an exact quantification of the speckle size versus scattering parameters, but it allows one to predict and explain its evolution. A better agreement between calculation and measurement was found further to the selection of the only photons involved in the speckle phenomenon.

#3393 - $15.00 US Received 20 November 2003; revised 19 December 2003; accepted 27 December 2003